




# Mapping of DDX11 genetic interactions defines sister chromatid cohesion as the major dependency

Leanne Amitzi,<sup>1</sup> Ecaterina Cozma <sup>2</sup>, Amy Hin Yan Tong,<sup>3</sup> Katherine Chan,<sup>3</sup> Catherine Ross,<sup>3</sup> Nigel O'Neil <sup>1</sup>, Jason Moffat <sup>3,4,5</sup>, Peter Stirling,<sup>2,\*</sup> Philip Hieter<sup>1,\*</sup>

<sup>1</sup>Michael Smith Laboratories, University of British Columbia, 2185 East Mall, Vancouver, British Columbia, V6T 1Z4, Canada

<sup>2</sup>Terry Fox Laboratory, BC Cancer Research Institute, 675 West 10th Avenue, Vancouver, British Columbia, V5Z 1L3, Canada

<sup>3</sup>Donnelly Centre, University of Toronto, Toronto, Ontario, M5S 3E1, Canada

<sup>4</sup>Department of Molecular Genetics, University of Toronto, Toronto, Ontario, M5S1A8, Canada

<sup>5</sup>Institute of Biomedical Engineering, University of Toronto, Toronto, Ontario, M5S3E1, Canada

\*Corresponding author: Michael Smith Laboratories, University of British Columbia, 2185 East Mall, British Columbia, Vancouver, V6T1Z4, Canada. Email: [hieter@mssl.ubc.ca](mailto:hieter@mssl.ubc.ca);

\*Corresponding author: Terry Fox Laboratory, BC Cancer, 675 West 10<sup>th</sup> Avenue, British Columbia, Vancouver, V5L1Z3, Canada. Email: [pstirling@bccrc.ca](mailto:pstirling@bccrc.ca)

DDX11/Chl1R is a conserved DNA helicase with roles in genome maintenance, DNA replication, and chromatid cohesion. Loss of DDX11 in humans leads to the rare cohesinopathy Warsaw breakage syndrome. DDX11 has also been implicated in human cancer where it has been proposed to have an oncogenic role and possibly to constitute a therapeutic target. Given the multiple roles of DDX11 in genome stability and its potential as an anticancer target, we set out to define a complete genetic interaction profile of DDX11 loss in human cell lines. Screening the human genome with clustered regularly interspaced short palindromic repeats (CRISPR) guide RNA drop out screens in DDX11-wildtype (WT) or DDX11-deficient cells revealed a strong enrichment of genes with functions related to sister chromatid cohesion. We confirm synthetic lethal relationships between *DDX11* and the tumor suppressor cohesin subunit *STAG2*, which is frequently mutated in several cancer types and the kinase *HASPIN*. This screen highlights the importance of cohesion in cells lacking DDX11 and suggests DDX11 may be a therapeutic target for tumors with mutations in *STAG2*.

**Keywords:** DDX11; helicase; synthetic lethality; cohesin; CRISPR

## Introduction

Synthetic lethality (SL) occurs when a sublethal genetic defect allows cell viability but leads to death if combined with a second sublethal genetic defect. Given the potential specificity of such interactions, SL is touted as a solution for genotype targeted precision anticancer therapeutics (Hartwell et al. 1997; O'Neil et al. 2017). The approval of poly-ADP ribose polymerase (PARP) inhibitors for the treatment of BRCA1/2-mutated advanced ovarian cancers and more recently for BRCA1/2-mutated breast cancers illustrates the potential of SL-based therapeutics (Bryant et al. 2005; Farmer et al. 2005; Kim et al. 2015). Cohesin is mutated across diverse cancer types, including glioblastoma, bladder cancer, acute myeloid leukemia, and Ewing's sarcoma (Solomon et al. 2014; Romero-Pérez et al. 2019). In total, this amounts to well over 100,000 Americans per year affected by a cohesin-mutated cancer, raising the possibility that cohesin-SL interactions could be impactful therapeutically. Previously, we screened for SL with mutant forms of cohesin subunits in yeast and identified a hub of SL targets, all associated with the stability of the replication fork (McLellan et al. 2009, 2012). One of the potentially druggable targets is the helicase Chl1 (the yeast ortholog of human DDX11 helicase).

DDX11 is a superfamily 2, an ATP-dependent DEAH/DEAD-box containing helicase belonging to the XPD-like helicase family, which contains 4 members (FANCF, XPD, RTEL1, and DDX11), all

having a conserved Fe-S-binding domain (Bharti et al. 2014). These proteins play important roles in genome stability and are implicated in rare genetic syndromes and cancer development (Wu et al. 2009; Suhasini and Brosh 2013). In vitro DDX11 unwinds DNA/DNA and DNA/RNA duplexes, as well as G-quadruplex (G4) structures with a preferred 5' to 3' directionality (Hirota and Lahti 2000; Farina et al. 2008; Wu et al. 2012; Bharti et al. 2013). DDX11 also interacts with Ctf18-RFC, PCNA, and FEN1 and stimulates FEN1 endonuclease activity on a flap DNA structure, a model intermediate substrate that forms during lagging strand synthesis (Farina et al. 2008).

Mutations in the yeast ortholog *chl1* result in elevated levels of chromosome loss or missegregation (Gerring et al. 1990; Holloway 2000). Chl1 plays a critical role during establishment of proper sister chromatid cohesion during S-phase and in DNA repair (Petronczki et al. 2004; Skibbens 2004; Ogiwara et al. 2007; Chung et al. 2011; Stoepker et al. 2015; Abe et al. 2018). In mammalian cells, depletion of DDX11 by shRNA/siRNA results in aneuploidy, abnormal sister chromatid cohesion, and a prometaphase delay leading to mitotic failure (Parish et al. 2006). DDX11 is required for proper chromosome cohesion at both centromeres and along the chromosome arms, and in its absence, cohesin complexes bind more loosely to chromatin (Inoue et al. 2007). In addition, it has been shown in both yeast and mammalian cells that Chl1/DDX11 binds to the replisome (in yeast via interaction with Ctf4

and in mammalian cells through interaction with Timeless) and that this interaction is required for effective sister chromatid cohesion (Samora et al. 2016; Cortone et al. 2018). In humans, bi-allelic mutations in *DDX11* cause the rare cohesinopathy-related disease, Warsaw breakage syndrome (WABS; van der Lelij et al. 2010). At the cellular level, fibroblasts and lymphoblasts cultured from WABS patients display increased spontaneous and drug-induced chromosomal breakage, sister chromatid defects, and sensitivity to drugs that impede replication [DNA cross-linking agent mitomycin C and topoisomerase I inhibitor camptothecin (CPT)] but not to drugs that elicit nucleotide excision repair or cause single- or double-stranded DNA breaks (such as X-ray and UV irradiation), supporting that *DDX11* plays a role in sister chromatid cohesion and replication fork stability or recovery, but not necessarily in repair of single-stranded or double-stranded DNA breaks (van der Lelij et al. 2010; Capo-Chichi et al. 2013).

In addition to identifying SL interactions, studying genetic interactions (GIs) can provide functional information on a protein's role and pathways (Kim et al. 2019). *DDX11* plays an important role in DNA replication, repair, and sister chromatid cohesion, and the yeast ortholog, *Chl1*, is a highly connected SL hub that interacts with many genes involved in cancer-relevant processes (Costanzo et al. 2016). However, the mammalian GIs of *DDX11* have not been widely studied, prompting our analysis of the *DDX11* SL interactome in this study. In this study, we conduct an unbiased genome-wide CRISPR/Cas9 knockout (KO) screen in isogenic *DDX11*-deficient human cells. We identified many genes involved in DNA replication, repair, and sister chromatid cohesion, supporting the key role that *DDX11* plays in linking DNA repair with establishment of sister chromatid cohesion and maintenance of genome stability. Our work supports another recent study using CRISPR screens in *DDX11* and *ESCO2* mutant cell lines that also shows a strong dependency of *DDX11*-deficient cells on cohesion regulators (van Schie et al. 2023).

## Materials and methods

### Cell lines

HAP1 cells are a near-haploid line derived from KBM-7 and have been previously described (Carette et al. 2011). HAP1 cells and HAP1 *DDX11* KO cells were cultured in Iscove's Modified Dulbecco's MFBS medium +10% fetal bovine serum (FBS) (Invitrogen) and incubated at 37°C and 5% CO<sub>2</sub>.

### Western blotting

Samples for western blot were lysed in Lysis buffer (50 mM Tris-HCl, pH 7.5, 150 mM NaCl, 10% glycerol, 1% Triton X-100, and protease inhibitors), sonicated, and debris spun down at ~18,000 × g at 4°C for 15 min. Samples were normalized by protein concentration using the bicinchoninic acid assay (BCA) (Thermo Fisher Scientific), run on 8% SDS-PAGE gels, and transferred to PVDF membrane (Immobilon-FL, Millipore). After probing with primary and secondary antibodies, blots were then subjected to ECL (Clarity or Clarity Max Western ECL substrate, BioRad) and visualized using a BioRad ChemiDoc MP Imager in the appropriate channel. Antibodies used for western blot were as follows: *DDX11* (1:1,000; Abnova, H00001663-B01P) and  $\alpha$ -tubulin (1:20,000; Abcam, ab18251). Secondary antibodies were either goat antimouse conjugated to HRP or goat antirabbit conjugated to HRP or Cy3 (Jackson Laboratories).

## Plasmids, primers, and single-guide RNA

For generation of KO lines, single-guide RNAs (sgRNAs; Table 1) were cloned into pSpCas9-T2A-blast, which was derived from pSpCas9-T2A-puro (Addgene # 62988). Blasticidin resistance gene was amplified from lenti-dCas9-VP64-blast (Addgene #61425) using primers OPH8968 and OPH8969 and cloned into the pCR-Blunt vector using Zero Blunt PCR Cloning Kit (Invitrogen) according to manufacturer's instructions. Site-directed mutagenesis to remove the BbsI site was performed using QuikChange Site-Directed Mutagenesis Kit (Agilent) and primers OPH9364 and OPH9365 and verified by Sanger sequencing. The modified blasticidin resistance gene was then cloned into pSpCas9-T2A-puro using EcoRI (replacing the puro gene) to obtain BPH1324. Finally, guide RNAs (gRNAs) were cloned into pSpCas9-T2A-blast using BbsI.

## Generation of clonal KO lines

HAP1 parent cells were transfected with BLA371+BLA332 (pSpCas9-T2A-Blast-*DDX11* Int. 5/6.2 + pSpCas9-2A-GFP-*DDX11* Intron 6/7.1) or BLA392 (pSpCas9-T2A-Blast-*DDX11* gRNA exon 4) plasmids using XtremeGene 9 (Roche) according to the manufacturer's instructions. The following day, transfected cells were selected using blasticidin (Sigma) for ~3 days, followed by replating at single-cell density in 10-cm plates. Ten to 14 days after plating, colonies were picked using cloning cylinders and transferred to a 96-well dish. Clones were passaged every 2–3 days until they reached 10 cm density, and *DDX11* protein KO was tested by western blot. Parent lines and *DDX11* KO clones were checked for mycoplasma before being used. Clones were also stained with propidium iodide (PI) and compared with parent cells by fluorescence-activated cell sorting (FACS) to determine ploidy.

To sequence the clones, due to the high identity between *DDX11* and other regions (*DDX12P* and *LOC642846*), genomic DNA was extracted using QuickExtract according to the manufacturer's instructions, and the relevant region was PCR amplified using primers OPH9318 + 9319 or OPH9320 + 9321 for HAP1 clones #1.1.5 and #2.1.5 and OPH9453 + 9454 for HAP1 clone #3.4.9. The PCR product was cloned into PCR\_Blunt and transformed into DH5 $\alpha$  cells, and ~10 colonies were sequenced for each clone using M13F and M13R primers.

## Drug sensitivity assays

Cells were plated in 100- $\mu$ L media in 96-well plates (6 wells per concentration). The next day, 100- $\mu$ L media containing CPT, olaparib, or hydroxyurea (HU, at 2 $\times$  final concentration) was added. Cells were incubated for further 3–4 days before being fixed in 3.7% paraformaldehyde and stained with Hoechst 33342, and nuclei were counted on a Cellomics Arrayscan VTI.

## CRISPR-Cas9 KO screen

CRISPR-Cas9 screen was performed as previously described (Aregger et al. 2020). Briefly, cells were infected with lentiviral TKOv3 library (a sequence-optimized sgRNA library of 71,090 sgRNAs targeting 18,053 human protein-coding genes with 4 sgRNAs per gene) at an MOI of ~0.3 such that each sgRNA was represented in about 200–300 cells and then selected the following day with puromycin (2  $\mu$ g/mL) for 48 h. Following selection, T0 samples were collected for determination of library representation at day 0, and the remaining cells were replated in 3 replicates maintaining >200-fold coverage of the library. Replicates were passaged every 3–4 days maintaining coverage of the sgRNA library and with 3 samples collected at T0 and all subsequent

**Table 1.** sgRNA, primers, and plasmids used in this study.

Identifier	crRNA
STAG2	/AltR1/rArUrU rUrCrG rArCrA rUrArC rArArG rCrArC rCrCrG rUrUrU rUrArG rArGrC rUrArU rGrCrU/AltR2/
HASPIN	/AltR1/rArCrC rGrUrG rArCrC rCrCrA rArGrA rCrGrC rCrUrG rUrUrU rUrArG rArGrC rUrArU rGrCrU/AltR2/
PAXIP1	/AltR1/rGrArGrGrUrCrArArGrUrArUrUrArCrGrGrGrUrGrUrUrUrUrArGrArGrCrUrArUrGrCrU/AltR2/
Identifier	Primers
OPH9318	AATGAGATGGGTGTGAAGAGCAGG
OPH9319	TCCCAATGCACAAAGCCGAG
OPH9320	AATGAGATGGGTGTGAAGAGCAGGG
OPH9321	GGAGACCAGCCGAACATCCT
OPH9453	ATTGTTCTGGGGCGATTCCG
OPH9454	GCACATAGCCAGTGAGGGTC
OPH8968	CTGGACATGCTGATTAACGAATTCGGCAGTGGAGAGGGCAGAG
OPH8969	CGATAAGCTTGATATCGAATTCTTAGCCCTCCACACATAAC
OPH9364	GCTGGCGACGCTGTAATCCTCAGAGATGGGGATG
OPH9365	CATCCCATCTCTGAGGATTACAGCGTCGCCAGC
Identifier	Plasmids
BPH1324	pSpCas9(BB)-2A-Puro (PX459) V2.0
BLA371	spCas9-T2A-Blast-DDX11 Int. 5/6.2-3
BLA332	spCas9-2A-GFP-DDX11 Intron 6/7.1-1
BLA392	spCas9-T2A-BLAST-DDX11 gRNA Exon 4-1

passages, until the infected population reached 16 doublings (T18). Genomic DNA was purified from T0 and endpoint samples using Promega Wizard Genomic DNA Purification kit according to the manufacturer's instructions. For each sample, sgRNA inserts were amplified from ~50 µg of genomic DNA by a 2-step PCR reaction using primers harboring Illumina TruSeq adaptors with i5 and i7 barcodes. The sequencing libraries were gel purified and sequenced on an Illumina HiSeq 2500. Log<sub>2</sub> fold changes (LFCs) and quantitative GI (qGI) scores were processed and calculated as in [Aregger et al. \(2020\)](#).

### Gene ontology term enrichment analysis

Enrichment of DDX11 GIs ( $|qGI| \geq 0.6$ , false discovery rate (FDR)  $\leq 5\%$ ) was analyzed using the PANTHER Overrepresentation Test (<https://geneontology.org/>) for either negative or positive interactions. The top 10 terms are shown for each of the hit categories.

### STAG2, HASPIN, and PAXIP1 knockdown and viability assays

The Alt-R CRISPR-Cas9 (from-integrated DNA technology [IDT]) system was used to generate STAG2, HASPIN, and PAXIP1 knockdown in HAP1 and DDX11 KO cell lines. Briefly, crRNAs targeting STAG2, HASPIN, or PAXIP1 (see [Table 1](#) for sequences) were mixed in equimolar ratios with tracrRNA (IDT) to form the sgRNA complex. A total of 1 µM sgRNA was complexed with 1 µM purified Cas9 (IDT), combined with RNAiMAX transfection reagent (Thermo Fisher Scientific) and mixed with cells.

HAP1 and DDX11 KO cells were seeded at 80,000 cells/well in a 24-well plate, reverse transfected as described above, and incubated for 48 h. Adherent cells were stained with crystal violet and resuspended in 10% acetic acid in methanol, and the OD570 was measured. HAP1 and DDX11 KO cells were reverse transfected as described above and seeded at 40,000 cells/well in an opaque 96-well plate and incubated for 48 h. A total of 150 µL of CellTiter-Glo reagent (Promega) were added to each well, and fluorescence intensity was measured at 520 nm.

HAP1 and DDX11 KO cells were seeded at 10,000 cells/well in a 24-well plate, incubated for 24 h, treated with CHR-6494 trifluoroacetate, and incubated for an additional 72 h. Adherent cells were stained with crystal violet and resuspended in 10% acetic acid in methanol, and the OD570 was measured.

## Results

### Generating DDX11 KO HAP1 clones

To generate DDX11 KO cell lines, we chose the human near-haploid cell line HAP1 as a model system, given the relative ease of generating KO mutations in this background ([Carette et al. 2011](#)). Targeting DDX11 is challenging as it is located in a complex repetitive region on chromosome 12. Several highly related DDX11 pseudogenes, including DDX12P and LOC642846, exist on chromosome 12, and members of the DDX11L family map to multiple chromosomes ([Amann et al. 1996](#); [Costa et al. 2009](#)). While we explored various strategies involving 1 or 2 sgRNAs ([Fig. 1a](#)), screening 47 clones for DDX11 protein KO, ultimately a single sgRNA strategy, produced clone 3.4.9. Clone 3.4.9 appeared to contain 2 editing events when aligned to DDX11 sequence (an insertion of a single C or insertion of CT—both of which create a frameshift and early termination). However, when aligning the sequences to DDX12P and LOC642846 pseudogenes as well as to DDX11, the single C insertion is most likely at the DDX11 locus, and the CT insertion is more likely to be at DDX12P or LOC642846 loci. Therefore, it seems that this clone was also derived from a haploid clone that diploidized after the genome editing event. This DDX11 KO in clone 3.4.9 appeared to be complete by western blot ([Fig. 1b](#)) and exhibited sensitivity to CPT and olaparib but not HU ([Fig. 1c](#)). This is consistent with published data that human lymphoblastoid cells lacking DDX11 are sensitive to CPT (a topoisomerase I inhibitor) and to PARP inhibitors, but DDX11/Chl1 is largely dispensable for cell survival in chicken DT-40 and budding yeast cells following exposure to HU (a ribonucleotide reductase inhibitor; [van der Lelij et al. 2010](#); [Laha et al. 2011](#); [Stoepker et al. 2015](#); [Abe et al. 2018](#)). HAP1 cells often contain a subpopulation of cells that spontaneously switch to a diploid state during normal culturing and often become fully diploid within 10–20 passages after CRISPR/Cas9 editing ([Beigl et al. 2020](#)). To test the ploidy of the DDX11 mutant clones, cells were stained with PI and compared with parental cells by FACS analysis. Several candidate KO clones, including 3.4.9, had become diploid compared with the parental line ([Fig. 1d](#)). In summary, clone #3.4.9 demonstrated the cleanest KO by western blot and the strongest expected DDX11 KO drug sensitivity and was selected for the CRISPR/Cas9 KO screen.

### Genome-wide CRISPR/Cas9 KO screen of DDX11-deficient cell lines

We conducted a genome-wide CRISPR/Cas9 screen using the TKOv3 gRNA library, which contains ~71,090 gRNAs that target

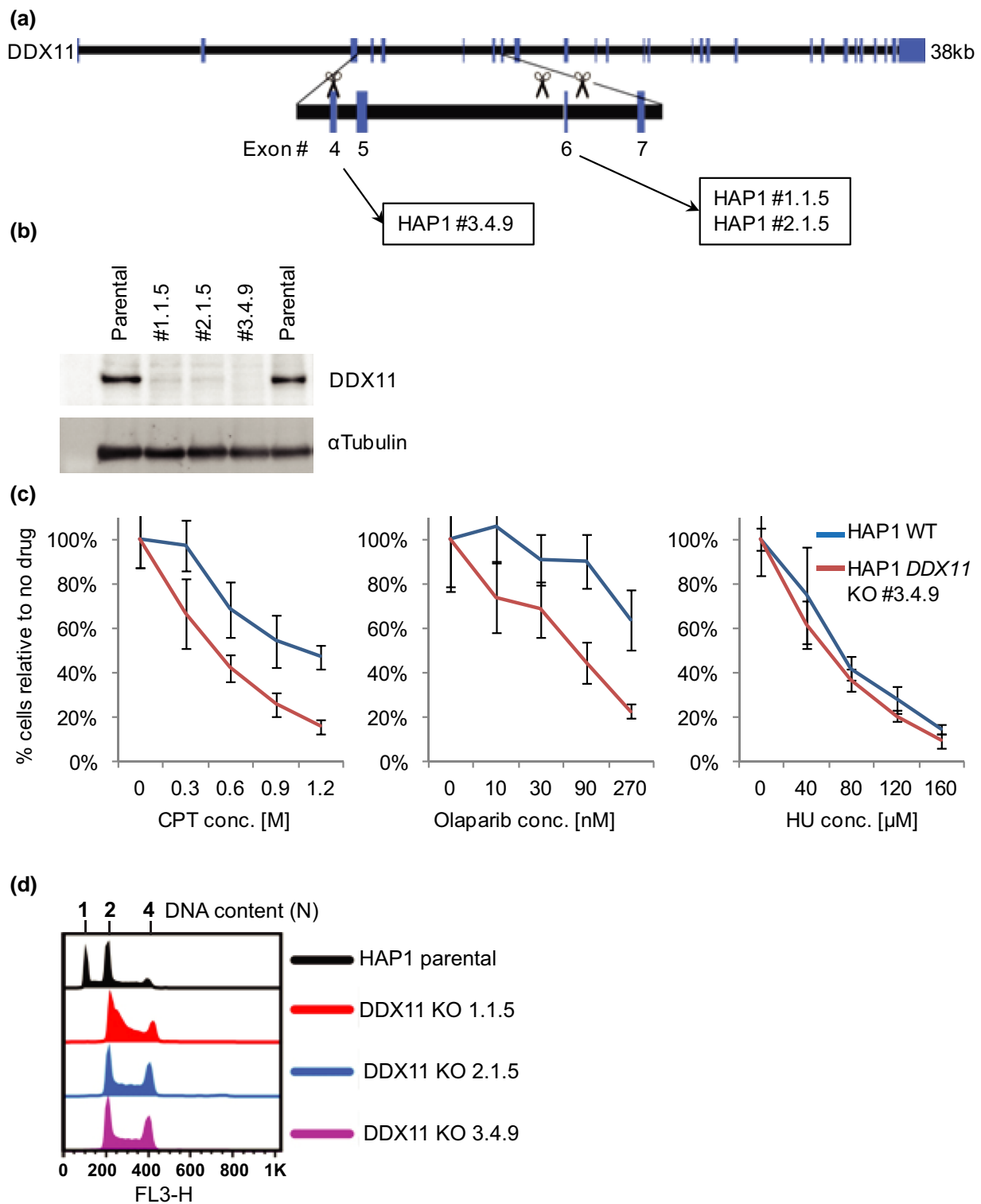


**Fig. 1.** Engineering DDX11 CRISPR/Cas9 KO lines. a) DDX11 genomic structure and strategy for making KO lines. Rectangular boxes represent exons, and the connecting lines represent intronic DNA. Scissors depict cleavage locations of sgRNAs selected, and boxes indicate which clones were derived from each strategy. b) Western blot analysis of DDX11 in promising HAP1 DDX11 KO clones. Alpha-tubulin is shown below as a loading control. c) HAP1 parental and lead candidate DDX11 KO cell lines treated with the indicated doses of CPT, olaparib (Ola), HU, or DMSO in 96-well format. After 3 days, cell numbers were quantified by nuclei counting using Cellomics Arrayscan VTI. Data are presented as mean  $\pm$  SD from 6 replicates. d) FACS analysis of PI-stained DNA content in the indicated cell lines to determine ploidy.

~18,000 human protein-coding genes, most of them targeted by 4 unique gRNAs (Hart et al. 2017; Aregger et al. 2019). The relative abundance of individual gRNAs was compared between the screen start (T0, following infection and selection) and end (T18,

after 16 doublings) providing an estimate of single-mutant fitness, whereas the relative abundance in DDX11-mutated cells provides an estimate of double-mutant fitness (schematized in Fig. 2a). The GIs were scored using a qGI score that measures the strength and

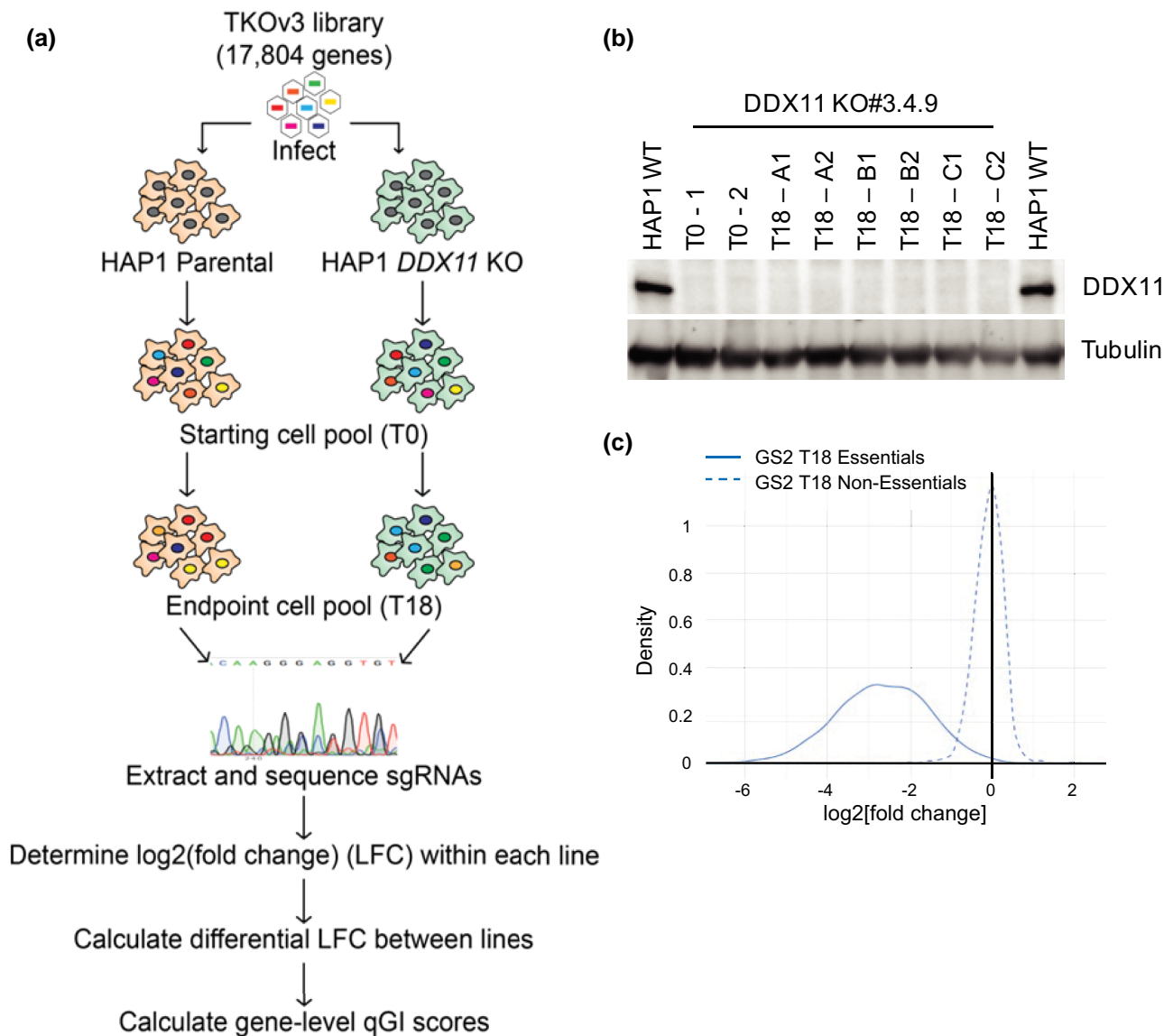


**Fig. 2.** CRISPR/Cas9 screen for the identification of GIs in DDX11 KO HAP1 cells. a) A schematic of the screen. DDX11 KO and WT parental cells were infected with a lentiviral genome-wide CRISPR gene KO library (TKOv3), and gRNA abundance was determined. LFC was calculated for each gRNA within each cell line, and then the differential LFC between WT and KO cells was calculated. Finally, a series of normalization steps and statistical tests were applied to these data to generate gene-level qGI scores and FDRs. b) Western blot of DDX11 from all cell lysates collected during and after the screen to confirm stable DDX11 KO. Tubulin is shown as a loading control. c) Screen quality control statistics showing differences in gRNA representation for core essential (solid) and nonessential (dotted) control genes targeted within the screen. Nonessential genes center around 0, while core essential genes appear strongly negative.

significance of the interaction by comparing the relative abundance of gRNA in the mutant cell line with the relative abundance of the same gRNA in an extensive panel of 21 wild-type HAP1 screens, after the removal of frequent flyers and batch correction (Aregger et al. 2019). Negative interactions reflect genes whose gRNAs are significantly decreased in the DDX11-mutated line relative to the control wild-type panel, whereas positive interactions reflect genes with increased gRNA abundance in DDX11-mutated line compared with the control wild-type panel.

DDX11 KO was maintained throughout the screen, and there was no reversion of the mutation to restore DDX11 levels (Fig. 2b). To evaluate screen performance, LFC of essential genes and non-essential genes were analyzed and compared with a reference set of core essential and nonessential genes as previously described (Hart et al. 2017). The screen robustly distinguished the reference set of essential genes from nonessential genes, indicating a high-

quality screen (Fig. 2c). Analysis of the DDX11 mutant-specific hits identified 324 negative GIs (NGIs) at a cutoff of  $qGI < -0.4$  at  $FDR \leq 0.2$  and 320 positive GIs (PGIs) at a cutoff of  $qGI > 0.4$  at  $FDR \leq 0.2$  for DDX11-KO cells. As expected, multiple genes associated with the cohesin complex and sister chromatid cohesion were identified as both positive and negative genetic interactors of DDX11-KO (Fig. 3). One of the strongest positive interactions was DDX11 itself, which supports the quality of the screen; gRNAs in the library targeting DDX11 cause impaired growth in the wild-type cells, but not the DDX11 KO cells as the protein is not expressed, and this manifests in the screen results as a positive interaction.

### Pathway analysis confirms cohesion-associated DDX11 dependencies

To provide further insight into the functional categories of genes identified, we performed gene ontology (GO) term enrichment

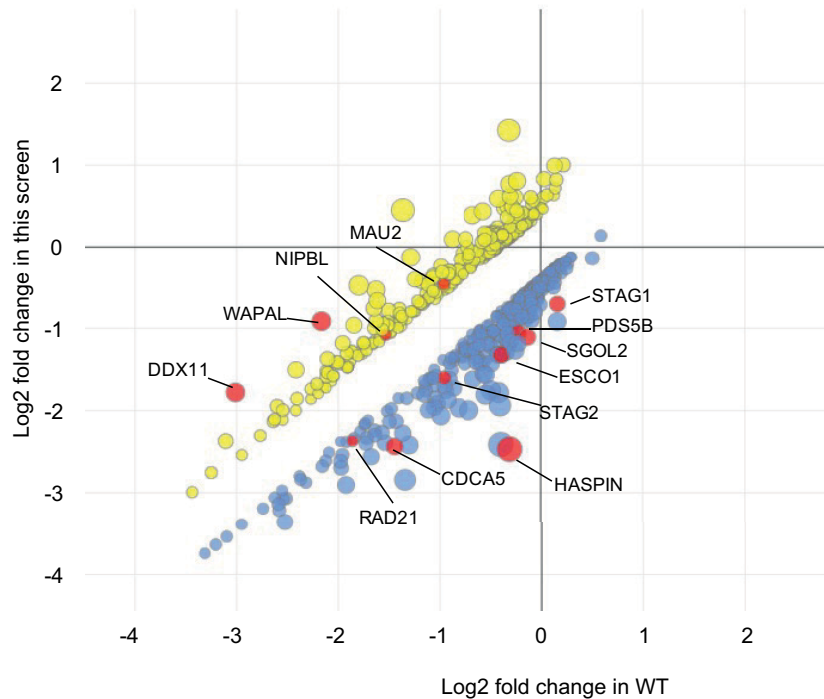


**Fig. 3.** DDX11 negative and positive GIs. A scatterplot illustrating the fitness effect (LFC) of 642 genes in DDX11 KO versus WT parental HAP1 cell line, which exhibited a significant GI ( $|qGI| > 0.4$ ,  $FDR < 0.2$ ). A total of 324 negative (blue, lower cluster) and 320 positive (yellow, upper cluster) DDX11 GIs are shown. Node size corresponds to a combined score reflecting both the qGI and the FDR. Selected genes belonging to the cohesin complex or affecting sister chromatid cohesion are highlighted in red (and labelled with lines and gene names).

analysis using PantherDB PANTHER Overrepresentation Test (Mi et al. 2021). We first looked at the negative GIs, which reflect genes that are SL or synthetic sick with DDX11 KO. For this analysis, we set a more stringent cutoff of  $qGI > 0.6$  to compute enrichments of the strongest hits. The top enriched terms for biological process GO terms are shown in Fig. 4a. Consistent with the known role of the DDX11 helicase, the enriched terms were associated with the cell cycle, DNA repair, and chromosome cohesion and segregation. Interestingly, among the top enriched terms that were associated with DNA damage response and cohesion related, supporting the hypothesis that DDX11 inhibition may be a good therapeutic target in cancer cells, many of which carry defects in DNA repair pathways.

A recent paper reported negative GIs for a DDX11 KO in immortalized RPE1 cell lines (van Schie et al. 2023). GIs are often context dependent with relatively few interactions conserved between different cell lines with the same genetic KO query gene. For example, a comparison of GIs with STAG2 KO in 3 different cell lines found only one interaction common to HAP1, RPE1, and tumor-derived H4 cell lines (Bailey et al. 2021). To find common GIs with loss of DDX11 and to corroborate the GIs found in the HAP1 CRISPR screen, we compared the top negative GIs reported by van Schie et al. (2023) with the top negative interactions found in our CRISPR screen. Of the 105 top negative interactions with DDX11 RPE1 (van Schie et al. 2023) and the 127 top negative interactions, we found in DDX11 KO HAP1 cells, 35 were common to both screens and were highly enriched for cohesion-associated genes (Fig. 4b).

### Validation of DDX11–cohesion GIs

Finally, we sought to confirm that the observed interactions could be reproduced by direct tests of fitness. We chose to focus on STAG2 because of its importance as a tumor-suppressor gene

lost in various cancers, PAXIP1 a recently identified cohesin regulator, and the Haspin kinase since it may be targetable with small molecules (Liang et al. 2018; Bailey et al. 2021; Mayayo-Peralta et al. 2023). We used CRISPR sgRNAs targeting STAG2, GSG2 (the catalytic subunit of Haspin), or PAXIP1 to generate knockdowns. Cellular fitness in gRNA transfected cells was measured in comparison with untreated or scrambled sgRNA controls using 2 independent assays. First, we quantified metabolically active cells using the CellTiter Glo cell viability assay and found that STAG2 and HASPIN sgRNA treatment significantly reduced cell viability in the DDX11-KO relative to a scrambled control but did not reduce fitness in the parental cell line (Fig. 5a). We also used crystal violet staining and colorimetric quantification as a proxy for cell viability. DDX11 KO cells were less viable/adherent compared with the parental lines (note the different Y-axis scales); however, treatment with the STAG2, HASPIN, or PAXIP1 sgRNA significantly reduced crystal violet staining in the KO but not in the wildtype (WT) cell lines (Fig. 5b). Finally, the HASPIN kinase inhibitor, CHR-6494 trifluoroacetate was tested and also qualitatively reduced the DDX11-KO cell growth compared with WT (Fig. 5c). Together, these experiments validate several cohesin-related hits from our primary screen, confirming that DDX11-KO cells are highly dependent on intact sister chromatid cohesion to survive.

### Discussion

Studying GIs expands our understanding of their molecular role(s) and therapeutic potential. The DDX11 helicase plays an important role in DNA replication, repair, and sister chromatid cohesion. The yeast DDX11 homolog, *CHL1*, is a highly connected SL hub with many genes involved in cancer-relevant processes, but the mammalian GIs of DDX11 are only recently being

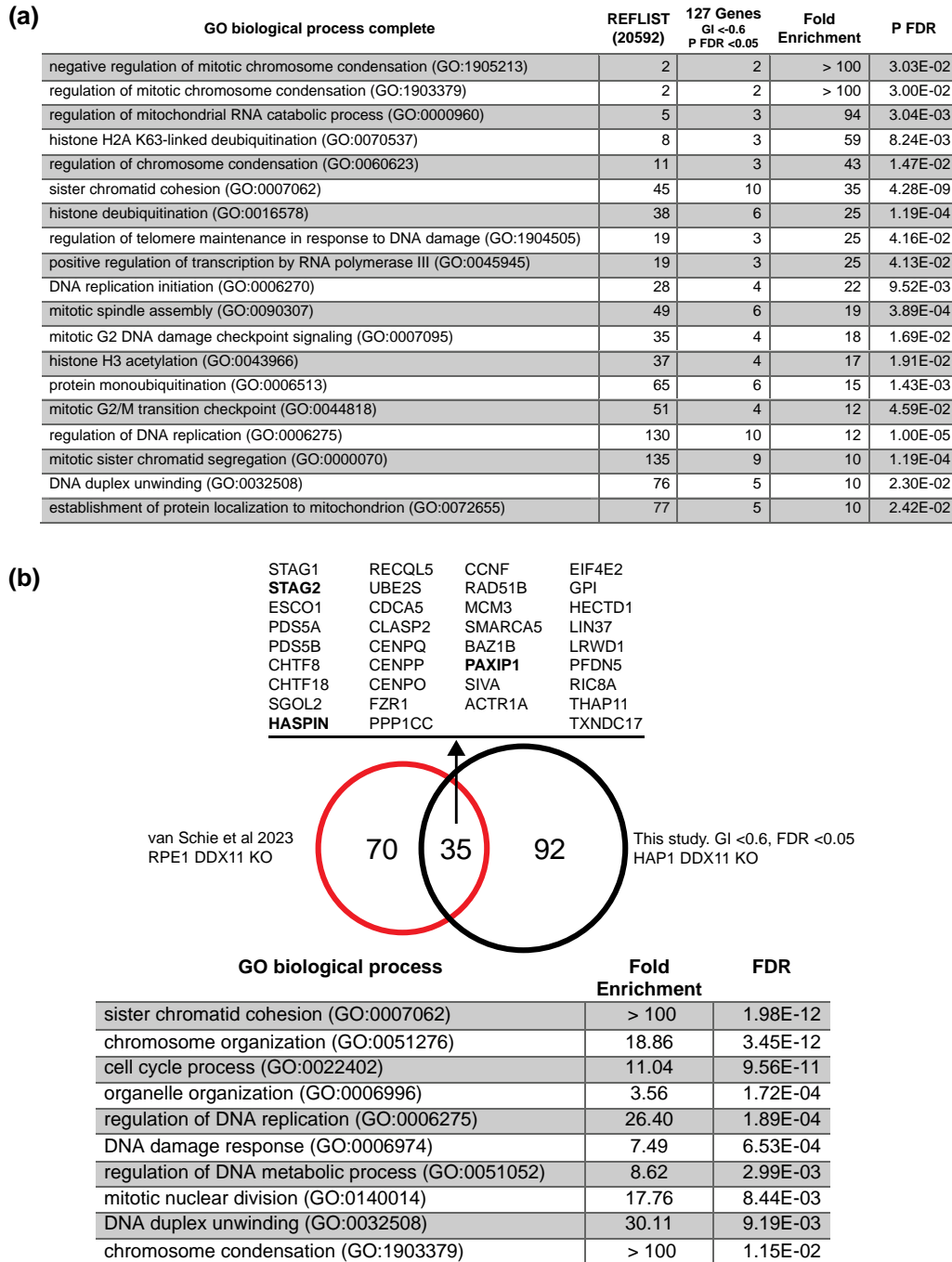


**Fig. 4.** The GO enrichment of dependencies and comparison of DDX11 GIs in HAP1 and RPE1 cell lines. a) A summary of top enriched biological processes ( $qGI > 0.6$ ,  $FDR < 0.05$ ) determined using the Panther DB (<https://geneontology.org/>). b) A comparative analysis of DDX11 GIs in HAP1 and RPE1 cell lines. GIs derived in the RPE1 cell line from van Schie et al. (2023) (smaller red circle). GIs derived in the HAP1 cell line in this study (larger black circle). Thirty-five negative GIs were shared between the experiments in HAP1 and RPE1. These shared interactions were enriched for cohesin, cell cycle, and DNA replication factors based on biological processes using the Panther DB (<https://geneontology.org/>).

defined (Faramarz et al. 2020; van Schie et al. 2023). The goal of this study was to conduct an unbiased screen in isogenic DDX11 KO cells to provide additional functional and therapeutic information.

For our screen, we chose to use HAP1 lines with/without DDX11. In a previous study, DDX11 was defined as an essential gene in HAP1 cells using a gene-trap method to systematically inactivate genes (Blomen et al. 2015). This essentiality is supported by data from the DepMap project (a large-scale project

aiming to systematically identify genetic and pharmacologic dependencies in a large panel of cancer lines), in which DDX11 is defined as a “common essential” gene (Pacini et al. 2021). Given the presence of highly similar DDX11 pseudogenes, it is possible that the “essentiality” of DDX11 in pooled CRISPR screens is, in part, a byproduct of multiple CRISPR-induced double-stranded breaks in the genome that reduce viability and are selected against in pooled competitive growth conditions. In the case of our generated clones, cells were edited and plated at single-

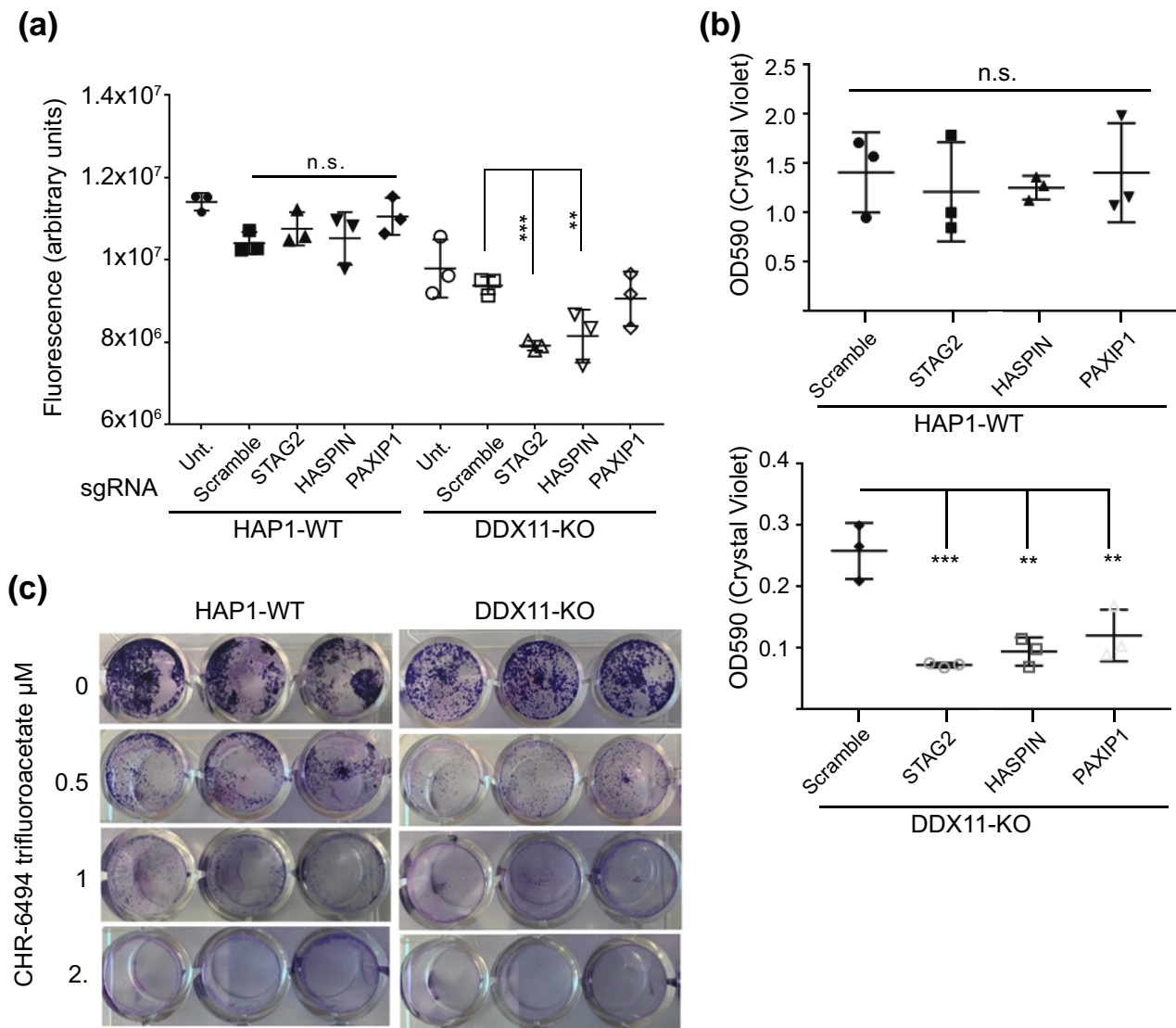


**Fig. 5.** The validation of CRISPR screen hit synthetic sickness with DDX11-KO. a) Cell viability by the CellTiter Glo method after transfection of the indicated gRNA. Each condition was measured in triplicate, and ANOVA was used to compare all means with the scramble-treated HAP1-WT cell line. \*\*\*\* $P < 0.0001$ , \*\*\* $P < 0.001$ , \* $P < 0.05$ . b) Crystal violet staining as a measure of viability in the indicated treatment conditions. Each condition was measured in triplicate, and the results of ANOVA comparing with the respective scramble treated are shown. \*\*\*\* $P < 0.0001$ , \*\*\* $P < 0.001$ , \*\* $P < 0.01$ . c) Crystal violet staining for viability of technical triplicates for the indicated cell line exposed to the indicated drug concentration of CHR-6494 trifluoroacetate.

cell density until the formation of a colony. Under these conditions, even cells with fitness defects may be able to survive and form colonies. Other groups have also managed to KO DDX11 in human cells in HeLa, U2OS, and RPE1 cells using CRISPR/Cas9 genome editing (Jegadesan and Brnzei 2021; van Schie et al. 2023).

Our screen identified multiple GIs (both positive and negative) with genes involved in sister chromatid cohesion or cohesion establishment and maintenance (Fig. 3). Our genetic screen was in a single-cell type, HAP1, and many GIs are cell line specific and are not broadly shared across cell lines. To identify common GIs with DDX11 KO, we compared our strong negative interactions with those from a CRISPR screen in immortalized retinal pigment epithelium (RPE) cells (van Schie et al. 2023). There was significant overlap (35/105 negative interactions) between the strong negative interactions, and the common interactions were enriched in genes involved in chromatin cohesion. This comparison reinforces the findings in both datasets.

The GIs observed reflect the underlying molecular roles of DDX11. For example, sororin (CDCA5), WAPAL, and PDS5 form a cohesin-regulator complex in vertebrates, in which sororin and WAPAL antagonize each other by competing for binding to a specific site on PDS5 to regulate association of cohesin with chromatin. This complex positively or negatively regulates the association of cohesin with chromosomes, depending on which protein binds to PDS5. PDS5-sororin complex maintains sister chromatid cohesion, whereas PDS5-WAPAL dislodges cohesin from chromatin (Zhang et al. 2021). In our screen, both CDCA5 and PDS5B were identified as negative GIs, whereas WAPAL was identified as a positive GI. This is consistent with the known role of DDX11 in establishing and maintaining sister chromatid cohesion. In the absence of DDX11, cohesion is less robust, and further dissociation through the loss of PDS5 or sororin may be detrimental to the KO cells. On the other hand, in wild-type cells, the loss of WAPAL is detrimental as it leads to increased cohesin on the DNA, whereas in the DDX11 KO cells, this effect is counteracted



by the loss of cohesion due to the loss of DDX11 activity. Another protein that ties into the regulation of cohesin maintenance versus removal is the kinase HASPIN (GSG2). HASPIN was one of the strongest negative GIs identified in the screen, and we confirmed the interaction with potent HASPIN kinase inhibitors. HASPIN binds and phosphorylates WAPAL, directly inhibiting the interaction of WAPAL with PDS5B. Cells expressing a WAPAL-binding-deficient mutant of HASPIN or treated with HASPIN inhibitors show centromeric cohesion defects (Liang et al. 2018). In contrast, HASPIN also binds to PDS5B, and KO of HASPIN or disruption of HASPIN-PDS5B interaction causes weakened centromeric cohesion and premature chromatid separation, which can be reverted by centromeric targeting of a short fragment of HASPIN containing the PDS5B-binding motif or by prevention of WAPAL-dependent cohesin removal (Zhou et al. 2017). Together, the interactions identified support a central role for DDX11 in regulation of cohesin establishment/protection versus removal.

One of the goals of this screen was to identify potential genetic features of tumors that might be treated with DDX11 inhibition. The pattern of interactions identified suggests DDX11 inhibition may be therapeutic for tumors exhibiting a cohesin-dysregulation/premature separation phenotype. This builds upon the concept of expanding the definition of clinically relevant SL from a gene/gene (or inhibitor) negative interaction to a phenotype or pathway + inhibitor interaction, similar to the recent evidence for expansion of PARP inhibitors from treatment of tumors carrying BRCA1/2 mutations to tumors displaying a “BRCAness” phenotype (Lord and Ashworth 2016).

In addition to potential therapeutic potential, studying GIs can provide information on the biological role of DDX11. This screen identified multiple genes important for sister chromatid cohesion, as well as genes involved in DNA repair, providing further support for the conservation of DDX11's role from yeast to human, and strengthening the idea of DDX11 inhibition as a therapeutic for cancer with cohesion defects. Of course, such cancers would need to be identified by the presence of a biomarker (similar to BRCA1/2 mutations as an indication for treatment with PARP inhibitors). Even in the absence of a defined genotypic vulnerability, such tumors could potentially be identified by a phenotypic assay of cohesion defects.

## Data availability

All data necessary to reach our conclusions are included within the manuscript and [Supplementary material](#). Unique reagents, cell lines, and other resources are available through contacting the corresponding authors.

[Supplemental material](#) available at G3 online.

## Funding

LA is supported by a Canadian Institutes of Health Research (CIHR) Vanier Canada Graduate Fellowship. EC is supported by a CIHR Canada Graduate Scholarship. This work was funded by grants from CIHR to PCS (project 398871), the Canadian Cancer Society Research Institute (grant number 704252) to PH and PCS, and the Canadian Institute for Advanced Research Genetic Networks Catalyst to PH and JM.

## Conflicts of interest

The author(s) declare no conflicts of interest.

## Literature cited

- Abe T, Ooka M, Kawasumi R, Miyata K, Takata M, Hirota K, Branzei D. 2018. Warsaw breakage syndrome DDX11 helicase acts jointly with RAD17 in the repair of bulky lesions and replication through abasic sites. *Proc Natl Acad Sci U S A*. 115(33):8412–8417. doi:10.1073/pnas.1803110115.
- Amann J, Valentine M, Kidd VJ, Lahti JM. 1996. Localization of chi1-related helicase genes to human chromosome regions 12p11 and 12p13: similarity between parts of these genes and conserved human telomeric-associated DNA. *Genomics*. 32(2):260–265. doi:10.1006/geno.1996.0113.
- Aregger M, Chandrashekar M, Tong AHY, Chan K, Moffat J. 2019. Pooled lentiviral CRISPR-Cas9 screens for functional genomics in mammalian cells. *Methods Mol Biol*. 1869:169–188. doi:10.1007/978-1-4939-8805-1\_15.
- Aregger M, Lawson KA, Billmann M, Costanzo M, Tong AHY, Chan K, Rahman M, Brown KR, Ross C, Usaj M, et al. 2020. Systematic mapping of genetic interactions for de novo fatty acid synthesis identifies C12orf49 as a regulator of lipid metabolism. *Nat Metab*. 2(6):499–513. doi:10.1038/s42255-020-0211-z.
- Bailey ML, Tieu D, Habsid A, Tong AHY, Chan K, Moffat J, Hieter P. 2021. Paralogous synthetic lethality underlies genetic dependencies of the cancer-mutated gene STAG2. *Life Sci Alliance*. 4(11):e202101083. doi:10.26508/lsa.202101083.
- Beigl TB, Kjosås I, Seljeseth E, Glomnes N, Aksnes H. 2020. Efficient and crucial quality control of HAP1 cell ploidy status. *Biol Open*. 9(11):bio057174. doi:10.1242/bio.057174.
- Bharti SK, Khan I, Banerjee T, Sommers JA, Wu Y, Brosh RM. 2014. Molecular functions and cellular roles of the ChlR1 (DDX11) helicase defective in the rare cohesinopathy Warsaw breakage syndrome. *Cell Mol Life Sci*. 71(14):2625–2639. doi:10.1007/s00018-014-1569-4.
- Bharti SK, Sommers JA, George F, Kuper J, Hamon F, Shin-ya K, Teulade-Fichou M-P, Kisker C, Brosh RM. 2013. Specialization among iron-sulfur cluster helicases to resolve G-quadruplex DNA structures that threaten genomic stability. *J Biol Chem*. 288(39):28217–28229. doi:10.1074/jbc.M113.496463.
- Blomen VA, Májek P, Jae LT, Bigenzahn JW, Nieuwenhuis J, Staring J, Sacco R, van Diemen FR, Olk N, Stukalov A, et al. 2015. Gene essentiality and synthetic lethality in haploid human cells. *Science*. 350(6264):1092–1096. doi:10.1126/science.aac7557.
- Bryant HE, Schultz N, Thomas HD, Parker KM, Flower D, Lopez E, Kyle S, Meuth M, Curtin NJ, Helleday T. 2005. Specific killing of BRCA2-deficient tumours with inhibitors of poly(ADP-ribose) polymerase. *Nature*. 434(7035):913–917. doi:10.1038/nature03443.
- Capo-Chichi J-M, Bharti SK, Sommers JA, Yamine T, Chouery E, Patry L, Rouleau GA, Samuels ME, Hamdan FF, Michaud JL, et al. 2013. Identification and biochemical characterization of a novel mutation in DDX11 causing Warsaw breakage syndrome. *Hum Mutat*. 34(1):103–107. doi:10.1002/humu.22226.
- Carette JE, Raaben M, Wong AC, Herbert AS, Obernosterer G, Mulherkar N, Kuehne AI, Kranzusch PJ, Griffin AM, Ruthel G, et al. 2011. Ebola virus entry requires the cholesterol transporter Niemann-Pick C1. *Nature*. 477(7364):340–343. doi:10.1038/nature10348.
- Chung G, O'Neil NJ, Rose AM. 2011. CHL-1 provides an essential function affecting cell proliferation and chromosome stability in *Caenorhabditis elegans*. *DNA Repair (Amst)*. 10(11):1174–1182. doi:10.1016/j.dnarep.2011.09.011.
- Cortone G, Zheng G, Pensieri P, Chiappetta V, Tatè R, Malacaria E, Pichierri P, Yu H, Pisani FM. 2018. Interaction of the Warsaw breakage syndrome DNA helicase DDX11 with the replication fork-

- protection factor Timeless promotes sister chromatid cohesion. *PLoS Genet.* 14(10):e1007622. doi:[10.1371/journal.pgen.1007622](https://doi.org/10.1371/journal.pgen.1007622).
- Costa V, Casamassimi A, Roberto R, Gianfrancesco F, Matarazzo MR, D'Urso M, D'Esposito M, Rocchi M, Ciccodicola A. 2009. DDX11L: a novel transcript family emerging from human subtelomeric regions. *BMC Genomics.* 10(1):250. doi:[10.1186/1471-2164-10-250](https://doi.org/10.1186/1471-2164-10-250).
- Costanzo M, VanderSluis B, Koch EN, Baryshnikova A, Pons C, Tan G, Wang W, Usaj M, Hanchard J, Lee SD, et al. 2016. A global genetic interaction network maps a wiring diagram of cellular function. *Science.* 353(6306):aaf1420. doi:[10.1126/science.aaf1420](https://doi.org/10.1126/science.aaf1420).
- Faramarz A, Balk JA, van Schie JJM, Oostra AB, Ghandour CA, Roommans MA, Wolthuis RMF, de Lange J. 2020. Non-redundant roles in sister chromatid cohesion of the DNA helicase DDX11 and the SMC3 acetyl transferases ESCO1 and ESCO2. *PLoS One.* 15(1):e0220348. doi:[10.1371/journal.pone.0220348](https://doi.org/10.1371/journal.pone.0220348).
- Farina A, Shin JH, Kim DH, Bermudez VP, Kelman Z, Seo Y-S, Hurwitz J. 2008. Studies with the human cohesin establishment factor, ChlR1: association of ChlR1 with Ctf18-RFC and Fen1. *J Biol Chem.* 283(30):20925–20936. doi:[10.1074/jbc.M802696200](https://doi.org/10.1074/jbc.M802696200).
- Farmer H, McCabe H, Lord CJ, Tutt AHJ, Johnson DA, Richardson TB, Santarosa M, Dillon KJ, Hickson I, Knights C, et al. 2005. Targeting the DNA repair defect in BRCA mutant cells as a therapeutic strategy. *Nature.* 434(7035):917–921. doi:[10.1038/nature03445](https://doi.org/10.1038/nature03445).
- Gerring SL, Spencer F, Hieter P. 1990. The CHL1 (CTF1) gene product of *Saccharomyces cerevisiae* is important for chromosome transmission and normal cell cycle progression in G2/M. *EMBO J.* 9(13):4347–4358. doi:[10.1002/j.1460-2075.1990.tb07884.x](https://doi.org/10.1002/j.1460-2075.1990.tb07884.x).
- Hart T, Tong AHY, Chan K, Van Leeuwen J, Seetharaman A, Aregger M, Chandrashekar M, Hustedt N, Seth S, Noonan A, et al. 2017. Evaluation and design of genome-wide CRISPR/SpCas9 knockout screens. *G3 (Bethesda).* 7(8):2719–2727. doi:[10.1534/g3.117.041277](https://doi.org/10.1534/g3.117.041277).
- Hartwell LH, Szankasi P, Roberts CJ, Murray AW, Friend SH. 1997. Integrating genetic approaches into the discovery of anticancer drugs. *Science.* 278(5340):1064–1068. doi:[10.1126/science.278.5340.1064](https://doi.org/10.1126/science.278.5340.1064).
- Hirota Y, Lahti JM. 2000. Characterization of the enzymatic activity of hChlR1, a novel human DNA helicase. *Nucleic Acids Res.* 28(4):917–924. doi:[10.1093/nar/28.4.917](https://doi.org/10.1093/nar/28.4.917).
- Holloway SL. 2000. CHL1 is a nuclear protein with an essential ATP binding site that exhibits a size-dependent effect on chromosome segregation. *Nucleic Acids Res.* 28(16):3056–3064. doi:[10.1093/nar/28.16.3056](https://doi.org/10.1093/nar/28.16.3056).
- Inoue A, Li T, Roby SK, Valentine MB, Inoue M, Boyd K, Kidd VJ, Lahti JM. 2007. Loss of ChlR1 helicase in mouse causes lethality due to the accumulation of aneuploid cells generated by cohesion defects and placental malformation. *Cell Cycle.* 6(13):1646–1654. doi:[10.4161/cc.6.13.4411](https://doi.org/10.4161/cc.6.13.4411).
- Jegadesan NK, Branzei D. 2021. DDX11 loss causes replication stress and pharmacologically exploitable DNA repair defects. *Proc Natl Acad Sci U S A.* 118(17):e2024258118. doi:[10.1073/pnas.2024258118](https://doi.org/10.1073/pnas.2024258118).
- Kim E, Dede M, Lenoir WF, Wang G, Srinivasan S, Colic M, Hart T. 2019. A network of human functional gene interactions from knockout fitness screens in cancer cells. *Life Sci Alliance.* 2(2):e201800278. doi:[10.26508/lsa.201800278](https://doi.org/10.26508/lsa.201800278).
- Kim G, Ison G, McKee AE, Zhang H, Tang S, Gwise T, Sridhara R, Lee E, Tzou A, Philip R, et al. 2015. FDA approval summary: olaparib monotherapy in patients with deleterious germline BRCA-mutated advanced ovarian cancer treated with three or more lines of chemotherapy. *Clin Cancer Res.* 21(19):4257–4261. doi:[10.1158/1078-0432.CCR-15-0887](https://doi.org/10.1158/1078-0432.CCR-15-0887).
- Laha S, Das SP, Hajra S, Sanyal K, Sinha P. 2011. Functional characterization of the *Saccharomyces cerevisiae* protein Chl1 reveals the role of sister chromatid cohesion in the maintenance of spindle length during S-phase arrest. *BMC Genet.* 12(1):83. doi:[10.1186/1471-2156-12-83](https://doi.org/10.1186/1471-2156-12-83).
- Liang C, Chen Q, Yi Q, Zhang M, Yan H, Zhang Bo, Zhou L, Zhang Z, Qi F, Ye S, et al. 2018. A kinase-dependent role for Haspin in antagonizing Wapl and protecting mitotic centromere cohesion. *EMBO Rep.* 19(1):43–56. doi:[10.15252/embr.201744737](https://doi.org/10.15252/embr.201744737).
- Lord CJ, Ashworth A. 2016. BRCAness revisited. *Nat Rev Cancer.* 16(2):110–120. doi:[10.1038/nrc.2015.21](https://doi.org/10.1038/nrc.2015.21).
- Mayayo-Peralta I, Gregoricchio S, Schuurman K, Yavuz S, Zaalberg A, Kojic A, Abbott N, Geverts B, Beerthuijzen S, Siefert J, et al. 2023. PAXIP1 and STAG2 converge to maintain 3D genome architecture and facilitate promoter/enhancer contacts to enable stress hormone-dependent transcription. *Nucleic Acids Res.* 51(18):9576–9593. doi:[10.1093/nar/gkad267](https://doi.org/10.1093/nar/gkad267).
- McLellan J, O'Neil N, Tarailo S, Stoepel J, Bryan J, Rose A, Hieter P. 2009. Synthetic lethal genetic interactions that decrease somatic cell proliferation in *Caenorhabditis elegans* identify the alternative RFC CTF18 as a candidate cancer drug target. *Mol Biol Cell.* 20(24):5306–5313. doi:[10.1091/mbc.E09-08-0699](https://doi.org/10.1091/mbc.E09-08-0699).
- McLellan JL, O'Neil NJ, Barrett I, Ferree E, van Pel DM, Ushey K, Sipahimalani P, Bryan J, Rose AM, Hieter P. 2012. Synthetic lethality of cohesins with PARPs and replication fork mediators. *PLoS Genet.* 8(3):e1002574. doi:[10.1371/journal.pgen.1002574](https://doi.org/10.1371/journal.pgen.1002574).
- Mi H, Ebert D, Muruganujan A, Mills C, Albu L-P, Mushayamaha T, Thomas PD. 2021. PANTHER version 16: a revised family classification, tree-based classification tool, enhancer regions and extensive API. *Nucleic Acids Res.* 49(D1):D394–D403. doi:[10.1093/nar/gkaa1106](https://doi.org/10.1093/nar/gkaa1106).
- Ogiwara H, Ui A, Lai MS, Enomoto T, Seki M. 2007. Chl1 and Ctf4 are required for damage-induced recombinations. *Biochem Biophys Res Commun.* 354(1):222–226. doi:[10.1016/j.bbrc.2006.12.185](https://doi.org/10.1016/j.bbrc.2006.12.185).
- O'Neil NJ, Bailey ML, Hieter P. 2017. Synthetic lethality and cancer. *Nat Rev Genet.* 18(10):613–623. doi:[10.1038/nrg.2017.47](https://doi.org/10.1038/nrg.2017.47).
- Pacini C, Dempster JM, Boyle I, Gonçalves E, Najgebauer H, Karakoc E, van der Meer D, Barthorpe A, Lightfoot H, Jaaks P, et al. 2021. Integrated cross-study datasets of genetic dependencies in cancer. *Nat Commun.* 12(1):1661. doi:[10.1038/s41467-021-21898-7](https://doi.org/10.1038/s41467-021-21898-7).
- Parish JL, Rosa J, Wang X, Lahti JM, Doxsey SJ, Androphy EJ. 2006. The DNA helicase ChlR1 is required for sister chromatid cohesion in mammalian cells. *J Cell Sci.* 119(23):4857–4865. doi:[10.1242/jcs.03262](https://doi.org/10.1242/jcs.03262).
- Petronczki M, Chwalla B, Siomos MF, Yokobayashi S, Helmhart W, Deutschbauer AM, Davis RW, Watanabe Y, Nasmyth K. 2004. Sister-chromatid cohesion mediated by the alternative RF-CCtf18/Dcc1/Ctf8, the helicase Chl1 and the polymerase- $\alpha$ -associated protein Ctf4 is essential for chromatid disjunction during meiosis II. *J Cell Sci.* 117(16):3547–3559. doi:[10.1242/jcs.01231](https://doi.org/10.1242/jcs.01231).
- Romero-Pérez L, Surdez D, Brunet E, Delattre O, Grünewald TGP. 2019. STAG mutations in cancer. *Trends Cancer.* 5(8):506–520. doi:[10.1016/j.trecan.2019.07.001](https://doi.org/10.1016/j.trecan.2019.07.001).
- Samora CP, Saksouk J, Goswami P, Wade BO, Singleton MR, Bates PA, Lengronne A, Costa A, Uhlmann F. 2016. Ctf4 links DNA replication with sister chromatid cohesion establishment by recruiting the Chl1 helicase to the replisome. *Mol Cell.* 63(3):371–384. doi:[10.1016/j.molcel.2016.05.036](https://doi.org/10.1016/j.molcel.2016.05.036).
- van der Lelij P, Chrzanoska KH, Godthelp BC, Roommans MA, Oostra AB, Stumm M, Zdzienicka MZ, Joenje H, de Winter JP. 2010. Warsaw breakage syndrome, a cohesinopathy associated with mutations in the XPD helicase family member DDX11/ChlR1. *Am J Hum Genet.* 86(2):262–266. doi:[10.1016/j.ajhg.2010.01.008](https://doi.org/10.1016/j.ajhg.2010.01.008).
- van Schie JJM, de Lint K, Molenaar TM, Moronta Gines M, Balk JA, Roommans MA, Roohollahi K, Pai GM, Borghuis L, Ramadhin AR,

- et al. 2023. CRISPR screens in sister chromatid cohesion defective cells reveal PAXIP1-PAGR1 as regulator of chromatin association of cohesin. *Nucleic Acids Res.* 51(18):9594–9609. doi:[10.1093/nar/gkad756](https://doi.org/10.1093/nar/gkad756).
- Skibbans RV. 2004. Ch11p, a DNA helicase-like protein in budding yeast, functions in sister-chromatid cohesion. *Genetics.* 166(1):33–42. doi:[10.1534/genetics.166.1.33](https://doi.org/10.1534/genetics.166.1.33).
- Solomon DA, Kim JS, Waldman T. 2014. Cohesin gene mutations in tumorigenesis: from discovery to clinical significance. *BMB Rep.* 47(6):299–310. doi:[10.5483/BMBRep.2014.47.6.092](https://doi.org/10.5483/BMBRep.2014.47.6.092).
- Stoepker C, Faramarz A, Rooimans MA, van Mil SE, Balk JA, Velleuer E, Ameziane N, te Riele H, de Winter JP. 2015. DNA helicases FANCM and DDX11 are determinants of PARP inhibitor sensitivity. *DNA Repair (Amst).* 26:54–64. doi:[10.1016/j.dnarep.2014.12.003](https://doi.org/10.1016/j.dnarep.2014.12.003).
- Suhasini AN, Brosh RM. 2013. Disease-causing missense mutations in human DNA helicase disorders. *Mutat Res.* 752(2):138–152. doi:[10.1016/j.mrrev.2012.12.004](https://doi.org/10.1016/j.mrrev.2012.12.004).
- Wu Y, Sommers JA, Khan I, De Winter JP, Brosh RM. 2012. Biochemical characterization of Warsaw breakage syndrome helicase. *J Biol Chem.* 287(2):1007–1021. doi:[10.1074/jbc.M111.276022](https://doi.org/10.1074/jbc.M111.276022).
- Wu Y, Suhasini AN, Brosh RM. 2009. Welcome the family of FANCF-like helicases to the block of genome stability maintenance proteins. *Cell Mol Life Sci.* 66(7):1209–1222. doi:[10.1007/s00018-008-8580-6](https://doi.org/10.1007/s00018-008-8580-6).
- Zhang N, Coutinho LE, Pati D. 2021. PDS5A and PDS5B in cohesin function and human disease. *Int J Mol Sci.* 22(11):5868. doi:[10.3390/ijms22115868](https://doi.org/10.3390/ijms22115868).
- Zhou L, Liang C, Chen Q, Zhang Z, Zhang B, Yan H, Qi F, Zhang M, Yi Q, Guan Y, et al. 2017. The N-terminal non-kinase-domain-mediated binding of Haspin to Pds5B protects centromeric cohesion in mitosis. *Curr Biol.* 27(7):992–1004. doi:[10.1016/j.cub.2017.02.019](https://doi.org/10.1016/j.cub.2017.02.019).

Editor: G. Brown